The effect of malondialdehyde is modified by simian virus 40 transformation in human lung fibroblast cells

S. A. Yates, M. F. Murphy and S. A. Moore[1]*

School of Pharmacy and Biomolecular Sciences, Liverpool John Moores University, Liverpool, L3 3AF, UK

*Corresponding author. E-mail: s.moore6@wlv.ac.uk

Footnote:

[1]Present address: School of Biology, Chemistry and Forensic Science, University of Wolverhampton, Wolverhampton, WV1 1LY, UK

Abstract

The effects of malondialdehyde (MDA), a product of oxidative stress, on normal lung fibroblast cells (MRC5) and transformed c ells (MRC5 SV2) showed differing responses between the two cell lines. MRC5 cells showed lower viability at low MDA concentrations (<250 µM) but had better viability at higher concentrations than the transformed cells. Both cell lines showed an increase in the number of micronuclei, nuclear size and a relocation of p53 to the nucleus with increasing MDA. The expression of p53 was higher in the MRC5 cells at 24 h; 2-8 fold induction *vs* 1-2.5 fold in the MRC5 SV2 cells, but reduced to almost zero at 48 h in the MRC5 cells. Mutation sequencing of the PCR products of a 689 bp region (residues 4640-5328) of the *TP*53 gene revealed MRC5 had more mutations than MRC5 SV2 cells (*n* = 21 and 11 respectively) and that they were predominantly insertions (MRC5 81%, MRC5 SV2 100%). A common mutation was observed in both cell lines; a G insertion at residue 4724 (*n* = 7) which could prove to be a mutational hotspot. These results indicate that the transformed cells are slower to respond to oxidative stress and/or mutagenic compounds. The mutation spectrum of predominantly frameshift mutations (insertions) suggests that oxidative stress plays a minimal role in smoking related lung cancer, but could be of greater importance to other lung diseases and cancer caused by exposures such as passive smokers, passive vapers and atmospheric pollutants.

Keywords: malondialdehyde, malondialdehyde-deoxyguanosine adducts, M_1dG adducts, oxidative stress, *TP*53, mutations

1. Introduction

Oxidative stress has been associated with the pathogenesis of a number of different diseases (Reuter et al., 2010), including cancer that results from mutations in DNA. In particular, malondialdehyde (MDA) is an endogenous source of oxidative stress (Del Rio et al., 2005) that is known to be mutagenic in human cells (Niedernhofer et al., 2003) and can enhance the effects of other chemicals (Feng et al., 2006). ¯MDA levels in human plasma are very variable with reported concentrations varying dependent upon the analytical technique, interindividual variation and the health status of an individual. A review of MDA levels in smokers (Lykkesfeldt, 2007) reported MDA ranges of 0-40 µM, whereas up to 5 mM MDA was reported in the plasma of anemic *H pylori* infected patients (Vijayan et al., 2007). Moreover, MDA reacts with guanosine in genomic DNA to form malondialdehyde-deoxyguanosine (M_1dG) adducts which have been shown to induce frameshift mutations and base pair substitutions as well as interstrand cross-links in DNA (Chaudhary et al., 1994). Lifestyle and environmental exposure can cause an increase in both MDA (Atasayar et al., 2004; Del Rio et al., 2005) and M_1dG adducts, with the latter found in many tissues including bronchial mucosa of smokers (Munnia et al., 2006), blood of pathology workers (Bono et al., 2010) and nasal epithelium of schoolchildren (Peluso et al., 2013). Thus, DNA adduct detection is an appropriate means of measuring exposure but needs to be linked to an effect e.g. mutations that ultimately lead to cancer as DNA damage may be repaired and be of little consequence to the cells.

Almost every type of human cancer exhibits DNA damage in one specific gene, the tumour suppressor *TP*53, with mutation rates varying from 10-100% for different cancer types (Rivlin et al., 2011; Hecht, 2008). Modification of the *TP*53 gene, and subsequently its associated *p53* protein, is a frequent genetic event leading to malignancy. Specific mutations of *TP*53 have been reported for skin tumours due to UV exposure (Ziegler et al., 1993), liver tumours from exposure to dietary aflatoxin B1 that showed a mutational hotspot at codon 249 (Montesano et al., 1997) and for lung cancer in smokers (Hernandez-Boussard and Hainaut, 1998). However, the spectrum of *TP*53 mutations is different for non-smokers, who account for 10-25% of lung cancer cases, and there is a need to study the mechanisms involved (Couraud et al., 2012). The main *TP*53 transcript is 2586 bases in length and includes a 5' UTR which covers exon 1, a large intron between exons 1 and 2, and the coding sequence from exons 2 to 11 (Xu-monette et al., 2012). Exon 1 was deleted in human ovarian cancer cells (Lane et al., 1995) so is worthy of further study. However, a bias has been observed in the mutation screening of the human *TP*53 gene, with the majority of studies focusing on the main coding regions (exons 2-11) and overlooking the 5'UTR exon 1 (Liu and Bodmer, 2006).

The aim of this study was to examine the effects of MDA on lung fibroblast cells that had an intact *TP*53 gene (MRC5 cells) and those with a transformed *TP*53 gene (MRC5 SV2 cells) where normal p53 expression has been altered due to transformation with simian virus 40 (SV40) (Huschtscha and Holliday, 1983). Transformation with SV40 causes a raft of effects on the cells including T antigen binding to p53 and Rb proteins and the subsequent effect on the cell cycle (Pipas, 2009), and SV40 is known to be oncogenic in humans (Shah 2007). Fibroblast cells are an appropriate model for lung diseases due to their ability to differentiate and migrate in response to damage within the surrounding tissues. A range of parameters were investigated following treatment of the two cell lines with MDA including examination of p53 levels and the mutations spectrum of a 689 bp

sequence that includes exon 1 of the *TP*53 gene and the 5' untranslated region (5'UTR). The latter is non-functional and considered as 'junk' DNA and, hence as discussed above, not studied extensively but may be involved in translational processes.

2. Materials and methods

2.1 Materials

Hyperladder II (including DNA loading buffer) was purchased from Bioline, London (UK); *TP*53 primers, p53 complementary DNA (cDNA) primers and glyceraldehyde-3-phosphate dehydrogenase (*GAPDH*) primers were purchased from Eurofins MWG Operon (Ebersberg, Germany); molecular-grade water and a PureLink messenger ribonucleic acid (mRNA) mini kit were from Life Technologies (Paisley, UK); RNasin Plus RNase inhibitor, GoScript reverse transcriptase and GoTaq 2-step RT-qPCR system were purchased from Promega (Southampton, UK); random hexamers were from Qiagen (Manchester, UK); ethylenediaminetetraacetic acid (EDTA) 500 mM solution, tris(hydroxymethyl)aminomethane (tris) were from Severn Biotech (Kidderminster, UK); glacial acetic acid, ethidium bromide, boric acid, deoxynucleotide (dNTP) mix and hydrogen peroxide (30% v/v) were purchased from ThermoFisher (Loughborough, UK).

Dimethyl sulphoxide (DMSO), Minimum Essential Medium (MEM), L-glutamine (200 mM), penicillin-streptomycin (10,000 units/ml and 10 mg/ml), non-essential amino acids (NEAA), phosphate buffered saline (PBS), trypan blue solution (0.4% w/v), trypsin/EDTA Solution (0.25%), thiazolyl blue tetrazolium bromide (MTT), 1,1,3,3-tetramethoxypropane (TMP), concentrated hydrochloric acid (HCl), potassium hydroxide (KOH), potassium chloride (KCl), 4',6-diamidino-2-phenylindole (DAPI - 10 mg/ml), methanol, ethanol, cytochalasin B, Reddymix PCR mastermix, GenElute mammalian genomic DNA mini prep kit, Annexin V-CY3 apoptosis detection kit, agarose, were purchased from Sigma-Aldrich (Gillingham, UK). MRC-5 pd30 (ECACC 05090501) and MRC-5 SV2 (ECACC 84100401) cell lines were obtained from Public Health England (Salisbury, UK).

2.2 Preparation of Malondialdehyde

A 100 mM stock solution of MDA was prepared with 0.1664 mL TMP in 4.69 mL HCl (0.1 M), incubated at room temperature (RT) for 40 min, neutralised with 4.69 mL KOH (0.1 M) and made up to 10 mL with water (Leuratti et al., 1999).

2.3 Cell Culture and Treatment with Malondialdehyde

Cells were cultured in T75 flasks in MEM supplemented with; 2 mM L-glutamine, 100units/mL penicillin/streptomycin and 1% NEAA, at 37 °C, in a 5% CO_2/95% air humidified atmosphere. To prepare cells for MDA treatment cells were removed from the flasks using trypsin-EDTA, pelleted (1,000 rpm for 5 min) and resuspended in 10ml MEM and seeded at 1 x 10^4 cells/cm^2 and left to attach for 24 h prior to subsequent treatments with MDA. The MDA solution was diluted in media for cell treatments (0-1000 µM) of 24 and 48 h. The concentration range used was similar to another study where up to 1 mM MDA was used (Li et al., 2006). Where possible, MDA treatments were the same for all analyses except where high levels were considered inappropriate due to cell viability or for comparison with typical biological levels (. A positive control was used in all treatments (H_2O_2; 50 or 100 µM). MDA treated cells were then subjected to the following methods of analysis.

2.4 Cell viability

Following treatment of cells with MDA (in 96-well plates), the cells were incubated with MTT reagent (5 mg/ml) for 3 h at 37 °C, in a 5% CO_2/95% air humidified atmosphere. Next, DMSO (100 µL) was added and the cells left to incubate for 30 min on a shaker plate, before the absorbance was read using a Spectramax 190 ROM microplate reader (540 nm).

2.5 Micronuclei and Nuclei Area

Enlarged nuclei have been observed frequently as an early carcinogen-induced change in cultured cells and *in vivo*. Therefore the effect of MDA on nuclear morphology/size was determined. Cells were cultured as described above and then seeded onto sterile glass coverslips (1 x 10^4 cells/cm^2) and left to attach for 24 hr (37 °C, in a 5% CO_2/95% air humidified atmosphere) and then treated with MDA. To preserve the nuclear morphology, MDA treated cells were incubated with cytochalasin B solution (1 mg/ml in DMSO diluted 1.5:100 in complete media) for 24 h. Next, the media was discarded and the cells washed in PBS (×3) and fixed: the microscope slides were placed in hypotonic solution (0.4% Na-citrate + 0.4% KCl in distilled water) containing 4% formaldehyde and incubated at 4 °C for 8 min, and then placed in hypotonic solution only. An equal volume of fixative (4:1 methanol:glacial acetic acid) was added slowly to the hypotonic solution whilst gently shaking. Next, 50% of the hypotonic/fixative mixture was removed and an equal volume of fixative added slowly. The hypotonic/fixative mixture was removed and 100% fixative was added for >1 min. The fixative was removed and the slides were air dried then incubated in DAPI (50 µg/ml in distilled water) for 15 min at RT and then washed (x5) in PBS. The slides were viewed using a Zeiss 510 META laser scanning confocal microscope (excitation 350 nm, emission 470 nm) and micronuclei identified. The area of 10 nuclei from each slide (repeated in triplicate for all MDA/H_2O_2 concentrations) were measured using ImageJ software (Rasband, 2016).

2.6 Apoptosis Detection

MDA treated cells were cultured for 24 h on glass coverslips (15 mm) placed in 12 well plates containing complete media. After 24 h the media was removed and the cells washed (x2) with PBS. Staining was carried out using the Annexin V-CY3 apoptosis detection kit according to the manufacturers' instructions (Sigma, UK). The cells were imaged using a Zeiss 510 META laser scanning confocal microscope.

2.7 *TP*53 Expression using Reverse Transcription Quantitative Polymerase Chain Reaction

MDA treated cells were recovered from the media, mRNA was extracted and purified using a PureLink RNA mini kit. The concentration of RNA was quantified using a NanoDrop spectrophotometer (260 nm), the samples diluted with RNase-free water and the RNA (0.463 µg) combined with random hexamers (final concentration 0.025 µg/µL random hexamers in 10 µL). Two negative controls were used: no RNA template and no reverse transcriptase with randomly chosen RNA samples. The tubes were incubated at 70 °C for 5 min, cooled to 4 °C for 5 min, centrifuged briefly and held on ice. A reverse transcription master mix was prepared on ice: 1.5 µL RNase-free water, 4 µL GoScript reaction buffer, 2 µL $MgCl_2$, 1 µL dNTP's, 0.5 µL RNase inhibitor, 1 µL reverse transcriptase per reaction mixture, and mixed thoroughly. 10 µL of the reverse transcription reaction mix was added to each RNA sample. cDNA was synthesized in a thermal cycler: annealed at 25 °C for

5 min, extended at 42 °C for 1 h, inactivated at 70 °C for 15 min, chilled at 4 °C then held ∞ or stored at -20 °C for later use.

A 1 µM stock solution of each primer were prepared using RNase-free water and held on ice. The *TP*53 cDNA primers were: forward 5'AGATGAAGCTCCCAGAATGC3' and reverse 5'TCTTGCGGAGATTCTCTTCC3'. *GAPDH* (reference gene) primers were: forward 5'GGTGAAGGTCGGAGTCAACGG3' and reverse 5'GGTCATGAGTCCTTCCACGAT3'. Primers were designed using Entrez Gene (Maglott et al., 2011), Primer3 (Untergasser et al., 2012) and primer BLAST bioinformatics (Ye et al., 2012).

A RT-qPCR reaction mix was prepared on ice, containing 10 µL GoTaq RT-qPCR Master Mix 2X, 4 µL RNase-free water and 1 µL each of either *TP*53 forward and reverse cDNA primers or *GAPDH* forward and reverse cDNA primers. Each RNA sample was prepared in triplicate, with 2 reactions per sample, one for *TP*53 and one for *GAPDH*, plus 2 reactions for the template-free control (*TP*53 and *GAPDH*) and 2 reactions for the reverse transcriptase-free control (*TP*53 and *GADPH*). RNA samples/control (4 µL) mixed with RT-qPCR reaction mix (16 µL) were centrifuged at low speed for 1 min. The RT-qPCR thermal cycler was programmed: activation at 95 °C for 2 min, 40 cycles of denaturation and annealing/extension for 95 °C for 15 s and 60 °C for 1 min, dissociation at 60-95 °C. SYBR was the detection dye and CXR was the reference dye. Expression of *TP*53 (target gene) relative to *GAPDH* expression was calculated using the $2^{-\Delta\Delta Ct}$ Comparative Cycle Threshold (Ct) method (Livak and Schmittgen, 2001). Samples were normalised to a RNA–free negative control and referenced against *GADPH*.

The RT-qPCR products were analysed on agarose gels (1%) prepared in Tris/Borate/EDTA (TBE) buffer (1.08 g tris base, 0.55 g boric acid and 0.4 mL 0.5 M EDTA (pH 8) in 100 mL H_2O) with 3 µL ethidium bromide. A marker (HyperLadder II, 500 – 2000bp) and samples (9 µL) were loaded into the wells with DNA loading buffer (1 µL). The electrophoresis was carried out at 95 V for 45 min to 1 h. The gels were viewed with a gel imager and BioRad Quantity One software.

2.8 Mutation sequencing of Polymerase Chain Reaction Products

Cells were treated with MDA for 48 h, and the DNA was extracted from the cells and purified using a GenElute Mammalian Genomic DNA Miniprep Kit. The DNA solutions were stored at -20 °C until required for PCR. Primers were designed using Ensembl (Flicek et al., 2011), Primer3 (Untergasser et al., 2012) and BLAST bioinformatics (Ye et al., 2012). The forward primer 5'TCTGGGAGAAAACGTTAGGG3' and reverse primer 5'ATCCCTCTAGCCAAGCTTCC3' flank residues 4640-5328 of the human *TP*53 gene (GenBank Accession Number NG_017013). A reaction master mix was prepared (25 µL ReddyMix PCR Mastermix, 0.5 µL each of forward and reverse primers, 19 µL molecular grade water per sample). DNA samples (5 µL) or negative control (H_2O) and reaction master mix (45 µL) were mixed and the PCR cycle performed: activation at 95 °C for 3 min, 40 cycles of denaturation, annealing and extension at 95 °C for 30 s, 57 °C for 1 min, 72 °C for 40 s, final extension at 72 °C for 5 min, then held at 4 °C. The products were checked by agarose gels (1%) prepared, and analysed, as described above with electrophoresis at 100 V for 30 min.

Sanger DNA sequencing was carried out on the unpurified PCR products (using the same primers as above) by Beckman Coulter Genomics (UK) by double stranded primer walking with an ABI Prism

3730XL DNA sequencer. The DNA sequences were analysed and processed using CLC Main Workbench 6 software (CLCBio, 2014). A consensus sequence combining both the forward and reverse sequences from each sample was created and aligned to the *TP*53 reference sequence and any unknown nucleotides were assigned. Conflicts between the *TP*53 reference sequence and the sample consensus sequence were identified and duplicate sample sequences were merged to include all possible mutations for that sample. A multiple alignment for each cell line was carried out, referenced to the *TP*53 reference sequence.

2.9 Statistics

All statistical analysis was carried out using Microsoft Excel 2007 software and results were significantly different if $P < 0.05$, unless otherwise stated.

3. Results

3.1 MTT Cell viability following MDA treatment

Initial concentrations of MDA were chosen across a large concentration range (0-1000 μM) in order to assess the effects of MDA on the relative viability of both cell lines. This range is similar to other studies (Li et al., 2006) but higher than typical biological levels of MDA in smokers (Lykkesfeldt, 2007) and was chosen to examine the effects across a broad range of concentrations as biological levels can be very variable (e.g. 5 mM in Vijayan et al., 2007). Figure 1 shows that both cell lines had an initial increase in viability after 24 h of treatment at low concentrations of MDA. Viability decreased to below 100% at 50 μM and 200 μM for the MRC5 and MRC5 SV2 cells respectively with viability dropping more noticeably in the MRC5 cells. However, for MRC5 the viability appears to stabilise at concentrations >300 μM whereas it continues to drop for MRC5 SV2 cells to lower than that of the MRC5 cells. A similar trend at low concentrations was observed at 48 h although the MRC5 cells had <100% viability at all MDA concentrations. At concentrations above 450 μM, the cell viability was very low in both cell lines (data not shown). The positive control (H_2O_2) showed a similar dose dependent decrease in cell viability (data not shown), but to a greater extent than MDA treatment. The percentage viability of MRC5 and MRC5 SV2 cells were compared with one another for each MDA concentration (0-450 μM) at 24 and 48 h. The viability of the two cell lines were found to be significantly different for MDA concentrations of ≥ 25 μM at 24 h (p = <0.0028). After 48 h, there was a significant difference in the viability of the two cell lines for the middle range of MDA concentrations (50-200 μM, p = <0.004). The low and high concentrations did not show a highly significant difference at 48 h (1-25 μM, p = 0.01, 250-450 μM, p = 0.002-0.016).

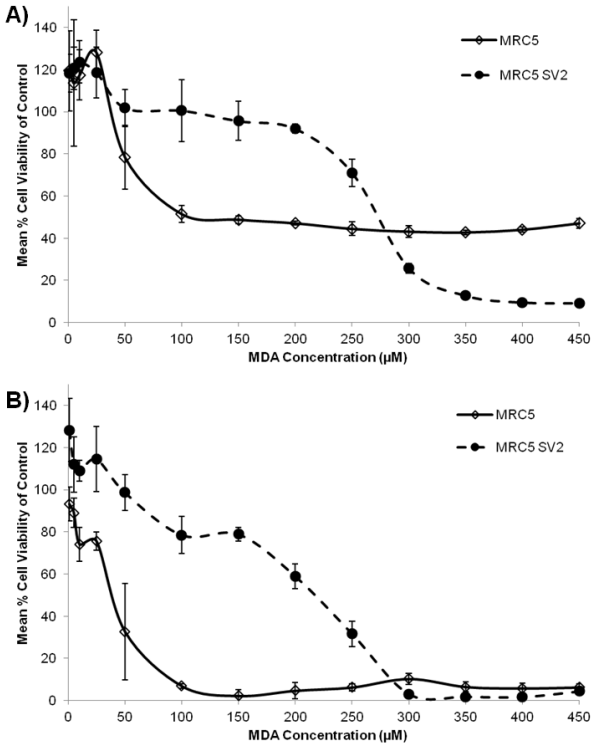

Figure 1 Viability of MRC5 and MRC5 SV2 cells treated with MDA (0-450 µM) over A) 24 h and B) 48 h, normalised to the negative control, error bars indicate ± 1SD from the mean (*n* = 4). Viability at >450 µM was very low (data not shown).

3.2 Formation of micronuclei

A modification of the micronucleus assay was utilised to examine nuclear morphology. DAPI-fluorescent images of cells treated with MDA are shown in Figure 2. As the concentration of MDA increases, the nuclei of both cell lines became more irregular in shape and what appear to be small fragments (possibly micronuclei) were observed in cells treated with 100 and 200 µM MDA. Little effect was observed on the nuclear morphology of cells treated with lower concentrations (10 and 50 µM; data not shown). The number of possible micronuclei observed appeared to increase with increasing MDA concentration, although very small fragments of DNA can also be seen in the negative controls, albeit to a lesser extent than treated cells.

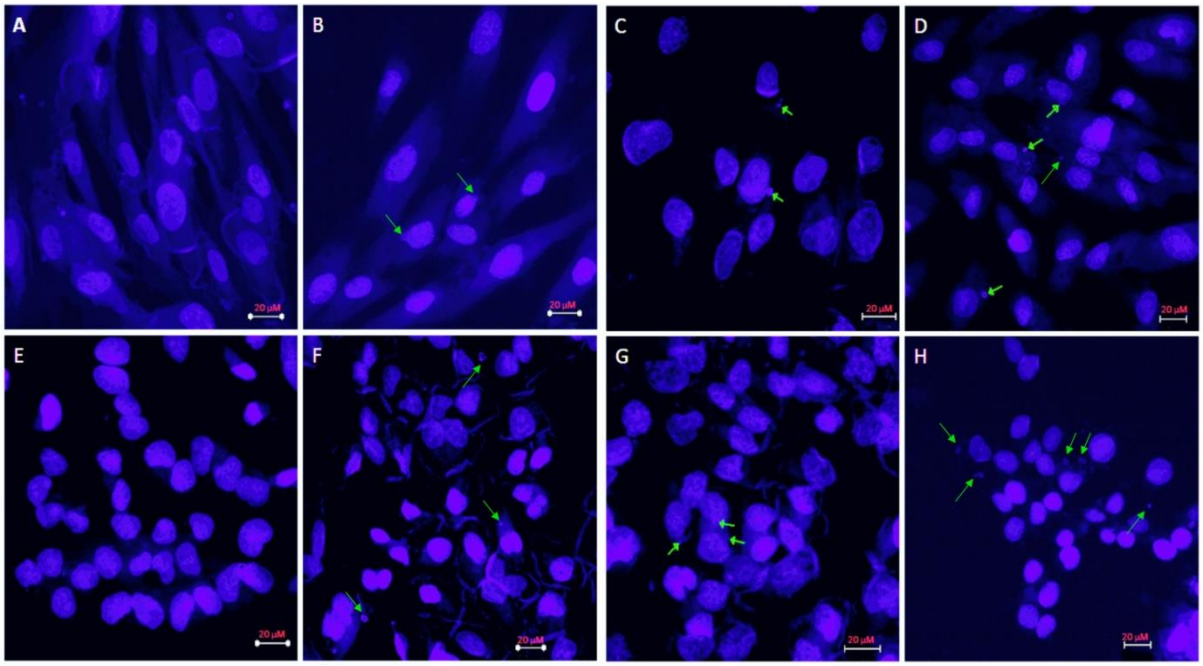

Figure 2 DAPI stain images of the nuclei of: A-D) MRC5 treated with MDA (left to right: 0, 50, 100 and 200 µM); and E-H) the corresponding images for MRC5 SV2 cells. A 10 µM treatment was also performed and was similar to the negative control (data not shown). The green arrows indicate possible micronuclei. Images are representative of sample replicates (*n* = 12). Scale bars = 20 µm.

3.3 Changes in nuclear area

To determine if there was any change in area of the nuclei following MDA treatment the mean areas of the nuclei were measured using ImageJ (Rasband, 2016). Figure 3 shows that the mean nuclear area of untreated MRC5 cells remained similar at 24 and 48 h. A general trend was seen in both cell lines with nuclear area increasing with an increase in MDA concentration, and also at 48 h compared with the same treatment at 24 h. Treatment with the positive control (50 µM H_2O_2; data not shown) for both cell lines showed a similar increase in nuclear area which was found to be significantly different when comparing MDA treatments at each time point. Single factor ANOVA analysis was performed on each cell line across all concentrations at a given time point. This revealed that the increases in nuclear size showed greater significance for the MRC5 SV2 cells than the MRC5 cells (p = 0.001 and 0.027 at 24 h and 48 h for MRC5, $p = 2 \times 10^{-6}$ and 3×10^{-4} at 24 h and 48 h for MRC5 SV2 respectively).

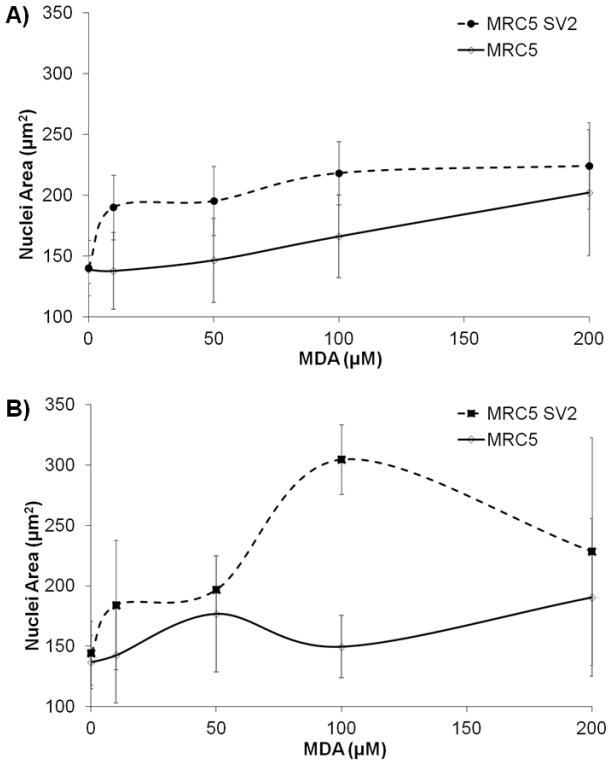

Figure 3 Area of nuclei of MRC5 and MRC5 SV2 cells treated with MDA (0-200 µM) over A) 24 h and B) 48 h, error bars indicate ± 1SD from the mean (*n*=10). The mean area was compared for all concentrations at both time points by ANOVA: MRC5 24 h, $p = 0.001$, 48 h $p = 0.027$; MRC5 SV2 24 h, $p = 2 \times 10^{-6}$, 48 h $p = 3 \times 10^{-4}$.

3.4 Apoptosis

To determine if MDA exposure triggers apoptosis in MRC5 and MRC5 SV2 cells a fluorescence apoptosis assay was carried out. This assay detects changes in membrane asymmetry which occur during the early stages of apoptosis. In this assay healthy cells fluoresce green, necrotic cells red and those in the early stages of apoptosis both red and green. Figure 4 shows selected MDA treatments whereby, after 24 h, the untreated cells (both MRC5 and MRC5 SV2) appeared to display predominantly green fluorescence indicating largely healthy cells. There is however some faint red fluorescence for the MRC5 SV2 cells which may indicate the background level of apoptosis in this population. The 10 µM treatment was very similar to the control in both cases, whereas the 200 µM treatment showed a much greater level of apoptosis (data not shown). Results for 48 h exposure to MDA and exposure with a positive control (100 µM H_2O_2) gave similar results to those shown in Figure 4 (data not shown).

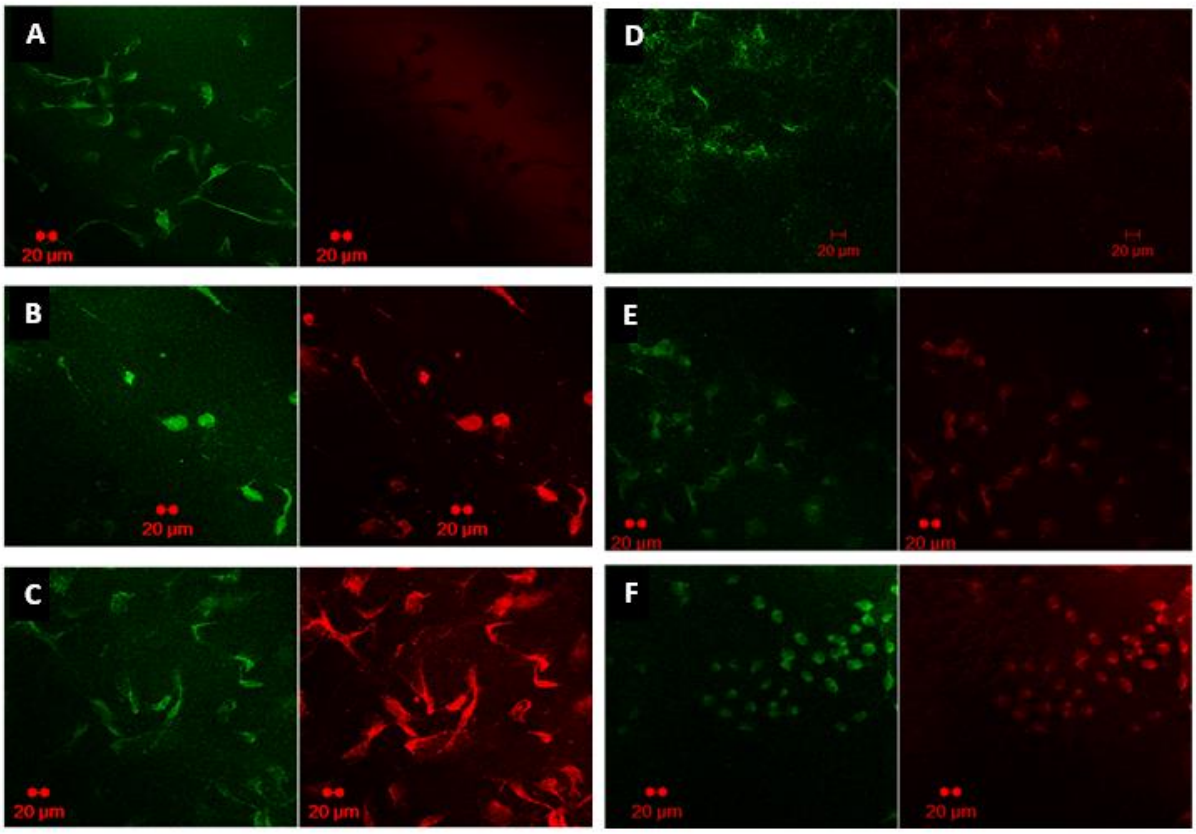

Figure 4 Apoptosis detection of selected MDA concentrations: A-C) MRC5 cells treated for 24 h with MDA (top to bottom: 0, 50, 100 µM); and D-F) the corresponding images for MRC5 SV2 cells. Imaging at x20 magnification using confocal microscopy. Red indicates cells stained for apoptosis and green for viable cells. Images are representative of each sample (*n* =6). The 10 and 200 µM data is not shown.

3.5 p53 expression

In order to determine if MDA induces an increase in p53 protein expression a fluorescence based assay was used. Overall, expression appeared to gradually increase in response to increasing MDA concentrations and treatment time with a slightly more intense fluorescence in the MRC5 SV2 cells than the MRC5 cells (Supplementary Figure 1). However, changes in colour intensity could not be reliably quantified so quantitative analysis of p53 protein expression levels was carried out to determine the relative levels in the two cell lines. Low concentrations of MDA (0 -100 µM), representative of normal biological ranges, were used in order to have sufficiently viable cells (see Figure 1). Ct values were measured for both p53 mRNA and GAPDH mRNA. The latter is a house-keeping gene, for which expression is assumed to remain constant (Barber et al., 2005), and was used as the reference gene to normalize the expression data to give the relative expression of p53 mRNA to GAPDH mRNA. This allows for any discrepancies in cell number and RNA extraction. The untreated (negative) control was used as a calibrator to which the treated samples were compared. The fold induction of p53 mRNA is shown in Figure 5. After 24 h treatment with MDA, p53 mRNA production was induced in both cell lines. Induction was greater at 10 µM MDA for MRC5 cells than

MRC5 SV2 cells and gradually decreased up to 100 µM MDA, whereas for MRC5 SV2 cells, induction increased at 50 µM MDA and decreased again at 100 µM MDA. After 48 h treatment, p53 mRNA induction was greatly reduced for MRC5 cells, as expected based on viability data (Figure 1), and only slightly reduced for MRC5 SV2 cells compared to 24 h treatment. In order to eliminate background noise due to amplification errors between samples, a cut-off point for fold induction should be applied. It has been suggested that the minimum fold change for significance is $\geq$ 2, with some studies suggesting up to 4 fold change as the cut-off point (Dalman et al., 2012). Application of the minimum cut-off point of a 2 fold induction to Figure 5 for the 24 h data would result in all data being statistically significant. Whereas, no results obtained after 48 h would be statistically significant, apart from MRC5 SV2 cells treated with 50 µM. Statistical comparison, using Student's t-test, of fold induction between the cell lines for each treatment showed no significant differences at 24 h (p >0.05). Whereas, at 48 h all treatments showed a significant difference between the two cell lines (p <0.006).

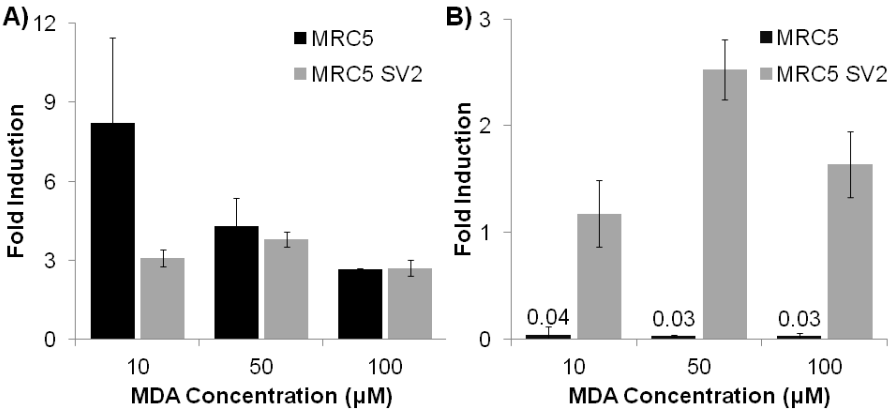

Figure 5 Induction of p53 mRNA expression relative to the negative control and reference gene GADPH, in cells treated with MDA (0 – 100 µM) for A) 24 h and B) 48 h, error bars indicate ± 1SD (n = 6). Values are indicated where induction was close to zero. Values of $\geq$ 2 fold induction are significant. Note the different scales on A and B.

3.6 Mutation sequencing of Polymerase Chain Reaction Products

DNA from MDA treated cells was extracted and a 689 bp section of the human *TP*53 gene was amplified by PCR and the resulting DNA sequence analysed. This included residues 4640-5328 of the 32,772 bp *TP*53 gene, located on chromosome 17 (GenBank accession NG_017013.2) (Clinvar RCV000079205.2, 2013). The sizes of the PCR products were checked by agarose gel electrophoresis and all had single bands at approximately 700 bp in size, corresponding to the PCR product length of 689 bp. The negative control, containing no DNA, had no band, whilst the positive control (H_2O_2) produced a single band corresponding to 689 bp (data not shown). PCR amplifies a DNA sequence and any damage to the DNA results in PCR products with an incorrect base compared to the original sequence. These incorrect bases are recorded as mutation to the original DNA sequence. Thus, the mutation sites and the type of mutations detected in the two MDA treated cell lines were compared to the same sequence from the *TP*53 gene (Table 1). In general, more mutations were observed in MRC5 DNA (n=21 MDA, n=20 H_2O_2) than for MRC5 SV2 DNA (n=11 MDA, n=12 H_2O_2). No mutations

occurred in the negative control DNA (untreated), nor in DNA where cells had been treated with 10 µM MDA. This may be due to very low levels of DNA damage and DNA repair mechanisms reversing any damage that may have formed, or that no DNA damage occurred in this relatively short section of DNA sequence under the conditions used. The number of mutations in the PCR products appears to peak at 100 µM MDA treatment for normal cells but there is no consistent pattern in the transformed cells. The data reveals some common mutations, notably a G insertion at residue 4724 (*n* = 7) whereas other common mutations showed a maximum of three occurrences. The mutation spectrum produced by H_2O_2 is very different to that by MDA with a higher number of transitions and tranversions in both cell lines, and very few common mutations showing the different effects of MDA and oxidative stress *per se*.

Table 1. Mutation type and position of mutations in DNA from MRC5 and MRC5 SV2 cells treated with MDA (10-1000 µM) and H_2O_2 (50-100 µM) for 48 h. Ins = insertion.

MDA	MRC5		MRC5 SV2		H_2O_2	MRC5		MRC5 SV2	
(µM)	Residue	Mutation	Residue	Mutation	(µM)	Residue	Mutation	Residue	Mutation
0	-	-	-	-	-	-	-	-	-
10	-	-	-	-	-	-	-	-	-
50	4821[a]	C → T	4724[f]	G ins	50	4714[i]	A → G	5215	G ins
	5149	G ins	-	-		4724[f]	G ins	-	-
	5152	G ins	-	-		5253[j]	T ins	-	-
						5263[h]	C ins	-	-
100	4738[b]	A → G	5253[j]	T ins					
	4823	T ins	-	-	100	4738[b]	A → G	4738[b]	A → G
	4832	C → A	-	-		4819	A → G	4788	T ins
	5188	T ins	-	-		4828	T → A	4791	G ins
	5216[c]	G ins	-	-		4830	A ins	4819	A → G
	5238	T ins	-	-		5150	G → C	4820	G → T
	5245	G ins	-	-		5209	A ins	4821[a]	C → T
	5254[d]	C ins	-	-		5214	G ins	4831	C → A
	5255[e]	T ins	-	-		5219	G → C	5046	A ins
						5224	A ins	5154	G ins
200	4724[f]	G ins	4724[f]	G ins		5226	G → A	5171	G ins
	5216[c]	G ins	5216[c]	G ins		5242	G → T	5287	G → A
	5256[g]	T ins	5256[g]	T ins		5260	G → T	-	-
	5263[h]	C ins	5263[h]	C ins		5266	G → T	-	-
						5281	G → T	-	-
500	4714[i]	A → G	5222	A ins		5287	G → A	-	-
	4724[f]	G ins	-	-		5311	G → T	-	-
	5255[e]	T ins	-	-					
1000	4724[f]	G ins	4724[f]	G ins					
	5254[d]	C ins	4725	A ins					
	-	-	5155	G ins					
	-	-	5253[j]	A ins					

[(a-j)]Indicates a repeat mutation

The type and percentage of mutations are summarised in Figure 6. In MRC5 cells treated with MDA, the majority of mutations were insertions, of which were mainly G, T and C (81% in total) but no A insertions. The remainder were transitions (A to G and C to T), and transversions (C to A). All of the mutations that occurred in the MRC5 SV2 cells were insertions (100%), of which the majority were G, but there were insertions of all bases including A which did not occur in the MRC5 cells. The positive control showed a greater variety of mutations than MDA treatments and a higher proportion of insertions in the MRC5 SV2 cells than their normal counterpart (68% *vs* 40%) as seen in the MDA treatments.

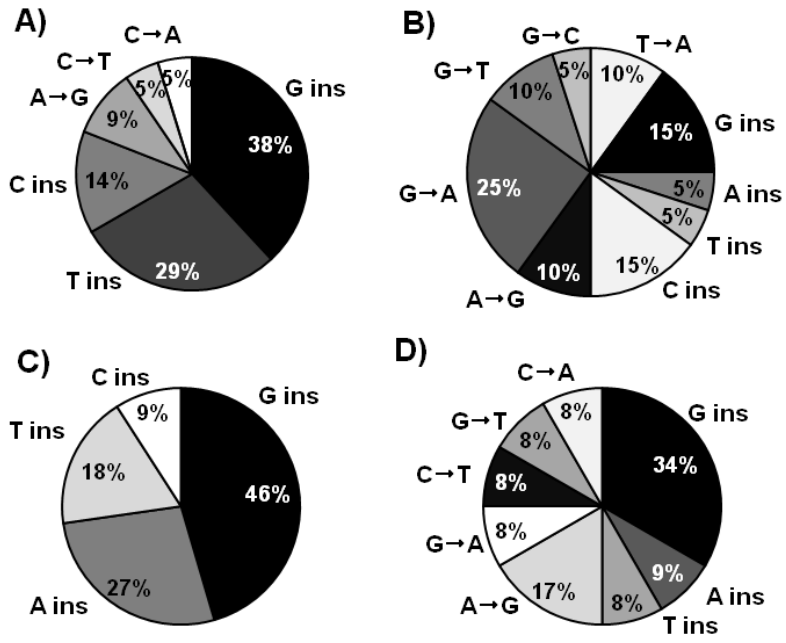

Figure 6 Type of mutations (%) in DNA from MRC5 cells treated for 48 h with A) MDA and B) H_2O_2 and MRC5 SV2 cells treated for 48 h with C) MDA and D) H_2O_2. MDA = 10-1000 µM and H_2O_2 = 50-100 µM.

4. Discussion

Comparison of the effect of MDA on the two cell lines was carried out with a focus on the impact on the *TP*53 gene and the p53 protein. Initial experiments on the effects of MDA showed the viability of the MRC5 cells decreasing more than that of the MRC5 SV2 cells at all concentrations (Figure 1), which is consistent with the MRC5 SV2 cells being transformed and hence lacking normal cell cycle control in response to toxic compounds (Huschtscha and Holliday, 1983). In general, the viability initially increased at low concentrations and then decreased after 24 h and with increasing MDA concentrations, and decreased further after 48 h for both cell lines, but to a greater extent with MRC5 cells. Similar trends have been observed in cell lines treated with other chemicals e.g. LL24 human fibroblast cells treated with benzene (Giuliano et al., 2009), and MRC5 cells and A549 human adenocarcinoma cells treated with cigarette smoke products (Liu et al., 2015), whereby low doses caused increased cell proliferation and higher doses were inhibitory. It was suggested that low doses cause defects in cell cycle control allowing increased proliferation as seen here.

Changes in the nuclei were observed in the form of both the appearance of micronuclei as MDA concentration increased (Figure 2) and the increase in the nuclear area (Figure 3). This was observed in both cell lines and indicates some reorganisation of the cytoskeleton, which may cause the cells to spread out and flatten. This would make the nucleus appear to be larger, or there may have actually been an increase in the volume of the nucleus. A similar observation was made in human primary diploid fibroblasts that had senesced, whereas apoptotic cells contracted and detached (Bladier et al., 1997). As the significance of treatment with MDA on nuclear area was lower at 48 h than 24 h, this may indicate that cells were starting to become apoptotic and beginning to contract. 3-D imaging and measurement of the nuclear volume would be required to confirm changes to nuclear size as opposed to flattening of the cells.

Apoptosis was seen to increase with MDA concentrations in both cell lines, albeit to a lesser degree in the MRC5 SV2 cells (Figure 4). Some cells were observed to be in the early stages of apoptosis, but still viable, and hence may have undergone reorganisation of the cytoskeleton which correlates with the changes seen in nuclear morphology. Thus it appears that transformation by SV40 reduced the level of apoptosis in this cell line which may be due to reduced activation of p53 dependent apoptotic factors or other factors such as pRb as mentioned earlier. The influence on p53 is consistent with a study of RKO (human colorectal carcinoma, wild type p53) and H1299 (human lung adenocarcinoma, p53-null) cells where MDA caused an increase in the apoptotic response with irreversible cell cycle arrest at G_1/S and G_2/M and elevation of p53 protein levels, and an increase in M_1dG adducts (Ji et al., 1998). Another study of human bone marrow mesenchymal stem cells found that increasing concentrations of MDA (up to 1 mM) decreased the cell count, increased the population doubling time, decreased cell viability and triggered apoptosis (Li et al., 2006), as observed here.

Increasing MDA gave an increase in p53 expression but also a change in the location of the protein (Supplementary Figure 1). p53 is synthesised in the cytoplasm and, when subject to cellular stress, p53 re-locates from the cytoplasm of the cell to the nucleus, where it is required to inhibit the growth of malignant cells (O'Brate and Giannakakou, 2003) At a low concentration, p53 was mainly in the cytoplasm where it is kept at low levels by interacting with Mdm-2 in unstressed cells, preventing transport to the nucleus. Increased levels of p53 protein were observed in the nuclei of cells treated with higher concentrations of MDA. This is consistent with cleavage of p53-Mdm-2 in response to stress, for example DNA damage, which activates p53 and is transported from the cytoplasm to the nucleus. There appears to be a greater effect for MRC5 SV2 cells than for MRC5 cells at 48 h which may be due to the sequestration of p53 in MRC5 SV2 cells causing a different response to their normal counterpart (Huschtscha and Holliday, 1983). Furthermore, quantitation of induction showed that p53 mRNA was increased to a greater extent at low concentrations compared to treatment with higher concentrations of MDA, and to a greater extent at 24 h than 48 h (Figure 5) which correlates with the qualitative observations. MRC5 SV2 cells continued to have induction of p53 mRNA after 48 h, albeit to a lesser extent than after 24 h, unlike the MRC5 cells. The difference in expression of p53 is clearly seen between the two cell lines with sequestration of p53 in MRC5 SV2 cells inducing the cells to express a greater amount of p53 to compensate for the bound p53. Studies of p53 expression in non-small cell lung carcinoma found high levels in 90% of tumours

(Cherneva et al., 2009), and increased p53 expression in human colon cancer cells treated with inositol hexaphosphate (Weglarz et al., 2006) although a decline in p53 mRNA expression was observed in human bronchial epithelial cells in response to treatment with aflatoxin B_1 (Van Vleet et al., 2006). Thus, there are differing cellular responses with regards to p53 expression dependant on the cause and site of the damage.

Mutation sequencing of the PCR products of DNA extracted from MDA treated cells showed almost double the number of mutations for MRC5 cells than the MRC5 SV2 cells (Table 1). In particular, the low concentrations (up to 100 µM) which are more representative of biological levels of MDA, showed more mutations in the normal cells than the transformed cells. The number of mutations in normal cells appears to increase up to 100 µM whereas the transformed cells do not show a dose-response relationship at any point. This may be due to the differing viabilities of the cells which showed that the transformed cells had much higher viability at low concentrations of MDA than normal cells, or that the cells respond in a number of different ways due to being transformed. Moreover, the type of mutations differed to those generated by hydroxyl radicals demonstrating the specific role of MDA. MRC5 showed predominantly insertions and some transitions and transversions whereas MRC5 SV2 cells exhibited only insertions (Figure 6). The predominant mutation was the G insertion at residue 4724, indicating a potential mutation hotspot in this DNA sequence. Exon 1 is located between residues 4953 and 5176 of the *TP*53 gene sequence, within the 689 bp region sequenced here. However, this region had only two mutations in the MRC5 cells and none in the MRC5 SV2 cells for MDA treatments, whereas the positive control did induce a few mutations in exon 1 of both cell lines. The 689 bp sequence examined aligns to residues 1841 to 1153 of the 17432 bp *Wrap53* gene sequence (Clinvar RCV000079205.2, 2013) in the antisense direction. Other studies have shown that MDA induces frameshift mutations and base pair substitutions (Benamira et al, 1995; Del Rio et al, 2005; Niedernhofer et al., 2003) as well as formation of M_1dG adducts. M_1dG is also mutagenic in mammalian cells, with the majority of mutations occurring as base substitutions and some frameshift mutations (insertions or deletions) (Stafford et al, 2009). Thus, there are several studies with similar mutations to those presented here. However, the presence of mutations detected by PCR and sequencing does not confirm that M_1dG adducts formed as the methodology used here involves PCR amplification of cellular DNA and therefore detects all mutations arising from damage to the DNA sequence rather than specific adduct formation. In the *TP*53 gene of lung cancer cells, the majority of mutations were transversions, of which there was a strong link between these types of mutation and cigarette smoking (Soussi et al., 2000), whereas there was an increase in transitions in *TP*53 lung cancer mutation spectra in non-smokers (Kim et al., 2012). However, an increase in frameshift mutations was observed in former or non-smokers who were exposed to passive smoking (Vähäkangas 2001) which correlates with the mutations found herein indicating that oxidative stress may play an important role in lung cancer associated with passive smokers. All of the aforementioned studies examined the main coding regions of *TP*53 (exons 2-11), whereas the region studied here has not been extensively studied previously (Liu and Bodmer, 2006). Hence, comparison of the type of mutations in lung fibroblast cells to other studies reveals that MDA mutations result in mainly frameshift mutations as seen in passive smokers (Vähäkangas 2001) rather than the mutation

spectrum seen in smokers. Furthermore, the mutation spectrum is modified by the status of the *TP*53 gene in the lung fibroblast cells used in this study.

5. Conclusion

The effect of MDA on the two lung fibroblast cell lines differed and the focus of the current study was on the effects on the *TP*53 gene and p53 protein. However, it is acknowledged that SV40 cell transformation induces a raft of other changes that may also affect the differing response of the cell lines It was found that MDA had a greater impact on the viability and p53 expression of normal cells as would be expected in response to a carcinogen, whereas transformed cells were slower to respond. Furthermore, the mutation spectra of the PCR products differed both in number and type. This indicates that transformed cells fail to respond appropriately to MDA exposure, or potentially other mutagens, which may result in higher levels of cancer and that this may be due to the altered response of the *TP*53 gene or other factors affected by SV40 transformation of the cells. The mutation spectrum differs from that seen in lung cancer cases suggesting that MDA, and hence oxidative stress, is not a major factor for lung cancer. However, an important finding of our study was that the predominant MDA-induced mutations in both cell lines were similar to those found in non-smokers and passive smokers (Vähäkangas 2001). MDA has long been associated with oxidative stress and, hence, the mutation spectrum observed herein has implications for future inhalation exposure studies such as in passive smokers or (passive) vapers, and other sources of inhalation such as environmental or occupational exposures.

Funding

This research did not receive any specific grant from funding agencies in the public, commercial, or not-for-profit sectors.

Conflicts of interest

There are no conflicts of interest to declare.

References

Atasayar, S., Orhan, H., Özgüneş, H., 2004. Malondialdehyde quantification in blood plasma of tobacco smokers and non-smokers. Fabad J. Pharm. Sci., 29**,** 15-19.

Barber, R.D., Harmer, D.W., Coleman, R.A., Clark, B.J., 2005. GAPDH as a housekeeping gene: analysis of GAPDH mRNA expression in a panel of 72 human tissues. Physiol. Genomics, 21**,** 389-395.

Benamira, M., Johnson, K., Chaudhary, A., Bruner, K., Tibbetts, C., Marnett, L.J., 1995. Induction of Mutations by Replication of Malondialdehyde-Modified M13 DNA in Escherichia-Coli - Determination of the Extent of DNA Modification, Genetic Requirements for Mutagenesis, and Types of Mutations Induced. Carcinogenesis, 16**,** 93-99.

Bladier, C., Wolvetang, E.J., Hutchinson, P., De Haan, J.B., Kola, I., 1997. Response of a Primary Human Fibroblast Cell Line to H_2O_2: Senescence-like Growth Arrest or Apoptosis? Cell Growth and Differentiation, 8**,** 589-598.

Bono, R., Romanazzi, V., Munnia, A., Piro, S., Allione, A., Ricceri, F., Guarrera, S., Pignata, C., Matullo, G., Wang, P., Giese, R.W., Peluso, M., 2010. Malondialdehyde-Deoxyguanosine Adduct Formation in Workers of Pathology Wards: The Role of Air Formaldehyde Exposure. Chem. Res. Toxicol., 23**,** 1342-1348.

Chaudhary, A.K., Nokubo, M., Reddy, G.R., Yeola, S.N., Morrow, J.D., Blair, I.A., Marnett, L.J., 1994. Detection of Endogenous Malondialdehyde-Deoxyguanosine Adducts in Human Liver. Science, 265**,** 1580-1582.

Cherneva, R.V., Georgiev, O.B., Petrov, D.B., Dimova, I.I., Toncheva, D.I., 2009. Expression levels of p53 messenger RNA detected by real time PCR in tumor tissue, lymph nodes and peripheral blood of patients with non-small cell lung cancer - new perspectives for clinicopathological application. Biotech. Biotech. Equipment, 23.

CLCBIO, 2014. CLC Main Workbench. www.clcbio.com.

Couraud, S., Zalcman, g., Milleron, B., Morin, F., Souquet P.-J., 2012. Lung cancer in never smokers – A review. Eur. J. Cancer, 48, 1299– 1311

Dalman, M.R., Deeter,A., Nimishakavi, G., Duan, Z.-H., 2012. Fold change and p-value cutoffs significantly alter microarray interpretations. BMC Bioinformatics, 13**,** S11.

Del Rio, D., Stewart, A.J., Pellegrini, N., 2005. A review of recent studies on malondialdehyde as toxic molecule and biological marker of oxidative stress. Nutr. Metab. Carbiovasc. Dis., 15**,** 316-328.

Feng, Z.H., Hu, W.W., Marnett, L.J., Tang, M.S., 2006. Malondialdehyde, a major endogenous lipid peroxidation product, sensitizes human cells to UV- and BPDE-induced killing and mutagenesis through inhibition of nucleotide excision repair. Mutat. Res.-Fundam. Mol. Mech. Mutagen., 601**,** 125-136.

Flicek, P., Amode, M.R., Barrell, D., Beal, K., Brent, S., Carvalho-Silva, D., Clapham, P., Coates, G., Fairley, S., Fitzgerald, S., 2011. Ensembl 2012. Nucleic Acids Res., 40**,** D84-D90.

Giuliano, M., Stellavato, A., Cammarota, M., Lamberti, M., Miraglia, N., Sannolo, N. and De Rosa, M., 2009. Effects of low concentrations of benzene on human lung cells in vitro. 188, 130–136.

Hecht, S.S. 2008., Progress and Challenges in Selected Areas of Tobacco Carcinogenesis. Chem. Res. Toxicol., 21**,** 160-171.

Hernandez-Boussard, T.M., Hainaut, P., 1998. A specific spectrum of p53 mutations in lung cancer from smokers: review of mutations compiled in the IARC p53 database. Environ. Health Perspect., 106**,** 385-391.

Huschtscha, L., Holliday, R., 1983. Limited and unlimited growth of SV40-transformed cells from human diploid MRC-5 fibroblasts. J. Cell Sci., 63**,** 77-99.

Ji, C., Rouzer, C.A., Marnett, L.J., Pietenpol, J.A., 1998. Induction of cell cycle arrest by the endogenous product of lipid peroxidation, malondialdehyde. Carcinogenesis, 19**,** 1275-1283.

Kim, S.-I., Yoon, J.-I., Tommasi, S., Besaratinia, A., 2012. New experimental data linking secondhand smoke exposure to lung cancer in nonsmokers. The FASEB Journal, 26**,** 1845-1854.

Lane, M.A., Abdellatif, N., Baunoch, D.A., Kaufman, L.M., Adelson, M.D., Reece, M.T., 1995. Deletion of *TP*53 exon-1 in human epithelial ovarian-cancer. Oncol. Rep., 2, 529-536.

Leuratti, C., Singh, R., Deag, E.J., Griech, E., Hughes, R., Bingham, S.A., Plastaras, J.P., Marnett, L.J., Shuker, D.E.G., 1999. A Sensitive immunoslot-blot assay for detection of malondialdehyde-deoxyguanosine in human DNA. In: Singer, B., Bartsch, H. (eds.) Exocyclic DNA Adducts in Mutagenesis and Carcinogenesis. Lyon: IARC.

Li, G., Li, H., Wang, B., Yin, D., 2006. Effects of malondialdehyde on growth and proliferation of human bone marrow mesenchymal stem cells in vitro. Front. Biol. China, 1**,** 131-136.

Liu, M., Poo, W.-K., Lin, Y.-L., 2015. Pyrazine, 2-ethylpyridine, and 3-ethylpyridine are cigarette smoke components that alter the growth of normal and malignant human lung cells, and play a role in multidrug resistance development. Exp. Mol. Pathol., 98**,** 18-26.

Liu, Y., Bodmer, W.F., 2006. Analysis of P53 mutations and their expression in 56 colorectal cancer cell lines. Proc. Natl. Acad. Sci. U.S.A., 103**,** 976-981.

Livak, K.J., Schmittgen, T.D., 2001. Analysis of relative gene expression data using real-time quantitative PCR and the $2^{-\Delta\Delta}$CT method. Methods, 25**,** 402-408.

Lykkesfeldt, J., 2007. Malondialdehyde as biomarker of oxidative damage to lipids caused by smoking. Clinica Chimica Acta 380: 50-58

Maglott, D., Ostell, J., Pruitt, K.D., Tatusova, T., 2011. Entrez Gene: gene-centered information at NCBI. Nucleic Acids Res., 39**,** D52-D57.

Montesano, R., Hainaut, P., Wild, C., 1997. Hepatocellular carcinoma: from gene to public health. J. Natl. Cancer Inst., 89**,** 1844-1851.

Munnia, A., Bonassi, S., Verna, A., Quaglia, R., Pelucco, D., Ceppi, M., Neri, M., Buratti, M., Taioli, E., Garte, S., Peluso, M., 2006. Bronchial malondialdehyde DNA adducts, tobacco smoking, and lung cancer. Free Radic. Biol. Med., 41**,** 1499-1505.

Clinvar RCV000079205.2, 2013, NCBI , National Center for Biotechnology Information, USA. https://www.ncbi.nlm.nih.gov/clinvar/RCV000079205/ (accessed 09/08/2018).

Niedernhofer, L.J., Daniels, J.S., Rouzer, C.A., Greene, R.E., Marnett, L.J., 2003. Malondialdehyde, a product of lipid peroxidation, is mutagenic in human cells. J. Biol. Chem., 278**,** 31426-31433.

O'Brate, A., Giannakakou, P., 2003. The importance of p53 location: nuclear or cytoplasmic zip code? Drug Resistance Updates, 6**,** 313-322.

Peluso, M., Munnia, A., Ceppi, M., Giese, R.W., Catelan, D., Rusconi, F., Godschalk, R.W.L., Biggeri, A., 2013. Malondialdehyde-deoxyguanosine and bulky DNA adducts in schoolchildren resident in the proximity of the Sarroch industrial estate on Sardinia Island, Italy. Mutagenesis, 28**,** 315-321.

Pipas, J.M., 2009. SV40: Cell transformation and tumorigenesis. Virology, 384**,** 294-303.

Rasband, W.S., 1997. ImageJ, U. S. National Institutes of Health, Bethesda, Maryland, USA,. https://imagej.nih.gov/ij/index.html 1997-2016 (accessed 23/11/2017)

Reuter, S., Gupta, S.C., Chaturvedi, M.M., Aggarwal, B.B., 2010. Oxidative stress, inflammation, and cancer: How are they linked? Free Rad. Biol. Med., 49, 1603-1616.

Rivlin, N., Brosh, R., Oren, M., Rotter, V., 2011. Mutations in the p53 Tumor Suppressor Gene: Important Milestones at the Various Steps of Tumorigenesis. Genes and Cancer, 2**,** 466-474.

Shah, K.V., 2007. SV40 and human cancer: A review of recent data. Int. J. Cancer, 120, 215-223.

Soussi, T., Dehouche, K., Beroud, C., 2000. p53 website and analysis of p53 gene mutations in human cancer: forging a link between epidemiology and carcinogenesis. Human Mut., 15**,** 105-113.

Stafford, J.B., Eoff, R.L., Kozekova, A., Rizzo, C.J., Guengerich, F.P., Marnett, L.J., 2009. Translesion DNA synthesis by human DNA polymerase n on templates containing a pyrimidopurinone deoxyguanosine adduct, 3-(2'-deoxy-β-D-erythro-pentofuranosyl)pyrimido-[1,2-α]purin-10(3H)-one. Biochemistry, 48**,** 471-480.

Untergasser, A., Cutcutache, I., Koressaar, T., Ye, J., Faircloth, B.C., Remm, M., Rozen, S.G., 2012. Primer3—new capabilities and interfaces. Nucleic Acids Res., 40**,** e115-e115.

Vähäkangas, K.H., Bennett, W.P., Castrén, K., Welsh, J.A., Khan, M.A., Blömeke, B., Alavanja, M.C.R., Harris, C.C., 2001. Mutations in Lung Cancers from Former and Never-Smoking Women. Cancer Res., 61**,** 4350-4356.

Van Vleet, T.R., Watterson, T.L., Klein, P.J., Coulombe, J.R.A., 2006. Aflatoxin B_1 alters the expression of p53 in cytochrome P450-expressing human lung cells. Toxicol. Sci., 89**,** 399-407.

Vijayan, G., Sundaram, R.C., Bobby, Z., Hamide, A., Selvaraj, N., Dasse, N.R., 2007. Increased plasma malondialdehyde and fructosamine in anemic H pylori infected patients: Effect of treatment. World J Gastroenterol., 13, 796–800.

Weglarz, L., Molin, I., Orchel, A., Parfiniewicz, B., Dzierzewicz, Z., 2006. Quantitative analysis of the level of p53 and $p21^{waf1}$mRNA in human colon cancer HT-29 cells treated with inositol hexaphosphate. Acta Biochimica Polonica, 53**,** 349-356.

Xu-Monette, Z.Y., Medeiros, J.L., Li, Y., Orlowski, R.Z., Andreeff, M., Bueso-Ramos, C.E., Greiner, T.C., Mcdonnell, T.J., Young, K.H., 2012. Dysfunction of the TP53 tumour suppressor gene in lymphoid malignancies. Blood, 119**,** 3668-3683.

Ye, J., Coulouris, G., Zaretskaya, I., Cutcutache, I., Rozen, S., Madden, T.L., 2012. Primer-BLAST: a tool to design target-specific primers for polymerase chain reaction. BMC Bioinformatics, 13**,** 134.

Ziegler, A., Leffell, D.J., Kunala, S., Sharma, H.W., Gailani, M., Simon, J.A., Halperin, A.J., Baden, H.P., Shapiro, P.E., Bale, A.E., 1993. Mutation hotspots due to sunlight in the p53 gene of nonmelanoma skin cancers. Proc. Natl. Acad. Sci. U.S.A, 90**,** 4216-4220.

Supplementary data

Method

p53 Expression

MDA treated cells were prepared as for apoptosis detection and the cells stained using a Cellomics p53 detection kit (ThermoFisher, Loughborough, UK). The cells were imaged using a Zeiss 510 META laser scanning confocal microscope.

Results and Discussion

In order to determine if MDA induces an increase in p53 protein expression a fluorescence based assay was use. Overall, expression gradually increased in response to increasing MDA concentrations (Supplementary Figure 1) and treatment time (data not shown) with a slightly more intense fluorescence in the MRC5 SV2 cells than the MRC5 cells. Treatment with the positive control (50 µM H_2O_2) also showed increased p53 expression over time (data not shown). Low levels of p53 protein were observed in the cytoplasm of both cell lines in the negative control and at 50 µM MDA, whereas following treatment with greater MDA concentrations (100-1000 µM), increased levels of p53 protein were observed in the nuclei indicating transport of the protein from the cytoplasm to the nuclei.

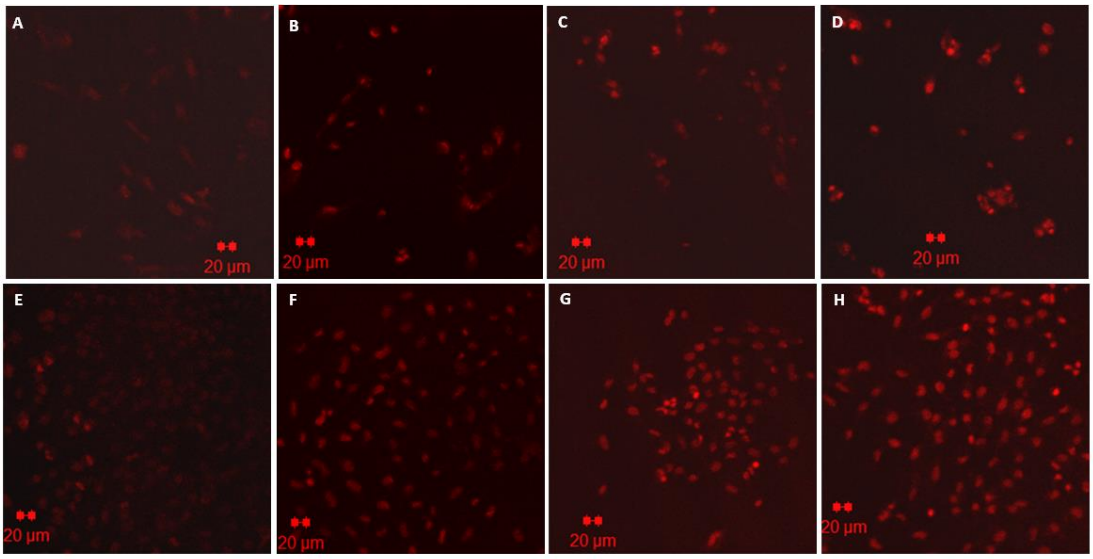

Supplementary Figure 1 p53 protein expression in: A-D) MRC5 cells treated for 48 h with MDA (left to right: 0, 200, 500 and 1000 µM) and E-H) the corresponding images for MRC5 SV2 cells. Cells stained red and imaged at x20 magnification.